


SCIENTIFIC REPORTS

There are amendments to this paper

OPEN

LRP1 is required for novobiocin-mediated fibronectin turnover

Natasha Marie-Eraïne Boel, Morgan Campbell Hunter & Adrienne Lesley Edkins 

Fibronectin (FN) plays a major role in the stability and organization of the extracellular matrix (ECM). We have previously demonstrated that FN interacts directly with Hsp90, as well as showing that the Hsp90 inhibitor novobiocin results in FN turnover via a receptor mediated process. However, the receptor involved has not been previously identified. LRP1 is a ubiquitous receptor responsible for the internalisation of numerous ligands that binds both Hsp90 and FN, and therefore we investigated whether LRP1 was involved in novobiocin-mediated FN turnover. FN, LRP1 and Hsp90 could be isolated in a common complex, and inhibition of Hsp90 by novobiocin increased the colocalisation of FN and LRP1. Novobiocin induced an increase (at low concentrations) followed by a loss of FN that was primarily derived from extracellular matrix-associated FN and led to a concomitant increase in intracellular FN. The effect of novobiocin was specific to LRP1-expressing cells and could be recapitulated by an LRP1 blocking antibody and the allosteric C-terminal Hsp90 inhibitor SM253, but not the N-terminal inhibitor geldanamycin. Together these data suggest that LRP1 is required for FN turnover in response to Hsp90 inhibition by novobiocin, which may have unintended physiological consequences in contexts where C-terminal Hsp90 inhibition is to be used therapeutically.

The extracellular matrix (ECM) is constantly remodelled to carry out functions involved in structural support and cell signalling¹. ECM homeostasis is maintained through a tightly controlled interplay between synthesis, deposition and degradation of matrix components, the deregulation of which has been linked to various pathological diseases^{2,3}. Among the ECM proteins, fibronectin (FN) plays important roles in cell adhesion, migration, wound healing and oncogenic transformation^{4,5}. FN is produced intracellularly as a soluble protein which is polymerized in an integrin-dependent mechanism into insoluble extracellular fibrillar structures that form the bulk of the ECM⁵⁻⁷.

Recently, Heat Shock Protein 90 kDa (Hsp90) was shown to regulate FN matrix stability⁸. Hsp90 is a ubiquitously expressed molecular chaperone which facilitates protein homeostasis in cells^{9,10}. Hsp90 is known to be upregulated in cancers and is required for the activation and maturation of oncogenic proteins¹¹⁻¹⁴. Hsp90 in the extracellular space mediates cell migration and contributes to metastasis^{12,15-18}. Hsp90 and FN interacted directly *in vitro* and in breast cancer cell lines, and Hsp90 depletion by RNA interference or inhibition with the C-terminal inhibitor novobiocin (NOV) induced FN internalisation by a receptor-mediated pathway⁸. However, the receptor mediating this turnover was not identified. LRP1 is a type I transmembrane receptor of the low density lipoprotein (LDL) receptor family¹⁹. LRP1 is known to be a scavenger receptor as it mediates the internalisation of a diverse range of ligands including proteinases, ECM proteins, bacterial toxins and viruses²⁰⁻²². Studies by Salicioni and colleagues have shown that FN accumulates in the extracellular space in LRP1-deficient CHO/MEF cells, and that LRP1 may serve as a catabolic receptor for FN²³. In addition to this role, LRP1 interacts with extracellular ligands to promote cell signalling to modulate cellular processes such as migration²⁴. Extracellular Hsp90 (eHsp90) is one such ligand of LRP1²⁵. Studies have demonstrated that eHsp90 utilizes a unique transmembrane signalling mechanism to promote cell motility and wound healing by binding to LRP1 and activating Akt kinases^{26,27}. Several groups have also reported roles for eHsp90 binding LRP1 in cell migration by activating various downstream signalling pathways including ERK, MMP2/9, NFκB^{26,28-34}.

The dynamics of FN matrix assembly and degradation play a large role in cell migration and invasion contributing to the metastatic potential of cancer cells. Thus, considering our previous study established a role for Hsp90 in FN matrix dynamics, and that both FN and Hsp90 interact with LRP1, we hypothesised that the LRP1 receptor was involved in the turnover of FN in response to Hsp90 inhibition by NOV. Herein, we report that a trimeric cell surface complex containing Hsp90, LRP1 and FN exists, and that LRP1 is required for the turnover of FN

Biomedical Biotechnology Research Unit, Department of Biochemistry and Microbiology, Rhodes University, Grahamstown, 6140, South Africa. Correspondence and requests for materials should be addressed to A.L.E. (email: a.edkins@ru.ac.za)

Received: 21 February 2018
Accepted: 13 July 2018
Published online: 30 July 2018

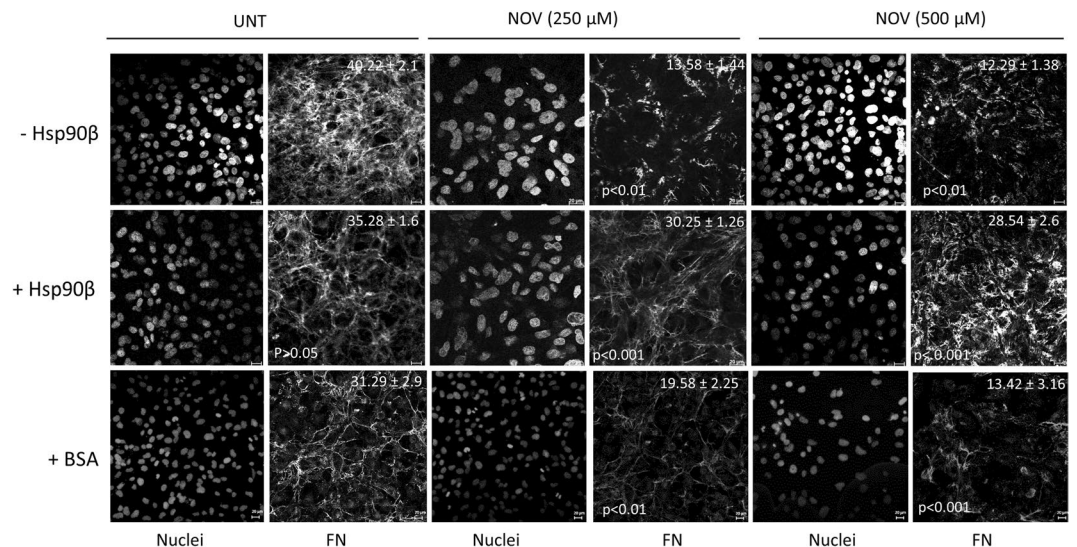


Figure 1. Treatment of Hs578T cells with NOV results in a loss of the FN matrix which is partially rescued by exogenous Hsp90β. Hs578T cells either remained untreated or were pre-treated with novobiocin (NOV; 250 or 500 μM) for 1 hour followed by addition of media with exogenous endotoxin-free Hsp90β (+Hsp90β; 100 ng/ml) or without (−Hsp90β) or with exogenous endotoxin-free BSA (+BSA; 100 ng/ml) overnight. Fixed cells were stained using mouse anti-human FN followed by donkey anti-mouse DyLight® 488 secondary antibody. Nuclei were stained with Hoechst 33342 (1 μg/ml). Images were captured using a Zeiss LSM 510 Meta laser scanning confocal microscope. Images were analyzed using Zen software, blue edition (Zeiss, Germany). Scale bars are equivalent to 20 μm. Values (in white) at the top of each frame represent the mean grey values per nuclei ± SD (n = 3) for each treatment. Mean grey values were compared using a one-way ANOVA with a Tukey Post Test. The mean grey value of NOV treatments (NOV; 250 or 500 μM) were compared to untreated cells for both negative controls (−Hsp90β and +BSA). The mean grey value of exogenous Hsp90β (+Hsp90β) treated cells were compared to the equivalent treatment with BSA (+BSA). Statistical p-values are shown in the bottom left of each frame. The data shown are representative of triplicate images collected from duplicate independent experiments.

upon Hsp90 inhibition with NOV. Whether Hsp90 acts to chaperone FN to LRP1 in this space or rather serves a cytokine-like role is still unclear.

Results

Loss of extracellular FN in response to NOV is rescued by Hsp90β. We first tested the effect of Hsp90 inhibition with NOV on the extracellular FN matrix. Hs578T breast cancer cells (which endogenously express high levels of FN matrix) were treated with or without increasing concentrations of NOV and the resulting FN phenotype observed. The ability of extracellular Hsp90 to rescue the observed phenotype was tested by addition of exogenous endotoxin-free Hsp90β (Fig. 1). Treatment with BSA, a non-specific protein that does not bind either LRP1 or NOV, served as a control for the addition of Hsp90β. The average FN fluorescence intensity per cell number (measured by the number of nuclei) in multiple images was quantified using ImageJ in order to compare the FN staining between samples. Hs578T cells showed a statistically significant and dose dependent decrease in the extracellular FN matrix upon treatment with increasing concentrations of NOV compared to the untreated (UNT) cells in both the presence of BSA (Fig. 1, bottom panel) and absence of Hsp90β (Fig. 1, top panel). There was a significant ($p < 0.001$) recovery of the extracellular FN matrix upon addition of exogenous Hsp90β to NOV treated cells (Fig. 1, middle panel). Treatment of Hs578T cells with Hsp90β alone showed no significant increase in the extracellular FN matrix, although better defined FN matrix fibrils were observed.

NOV increased colocalisation of FN and LRP1. As both Hsp90 and FN interact with LRP1, and the Hs578T cell line expresses LRP1, we hypothesised that this receptor may be involved in Hsp90-mediated FN turnover. We therefore investigated whether LRP1 colocalised with FN (Fig. 2) and/or Hsp90 (Fig. 3) and/or the lysosomal marker LAMP-1 (Fig. 4) in NOV-treated cells by confocal microscopy. In addition to the Hs578T cell line, we also used an isogenic mouse embryonic fibroblast (MEF) model system of differential LRP1 expression^{35,36}. The MEF1 cell line is derived from wild type mice, while the PEA13 cell line is isogenic lines from LRP1 knockout mice. Colour Scatter Plots generated shows plots of green intensities vs. red intensities with yellow indicative of overlapping green and red pixels. In both MEF-1 and Hs578T cells, increasing NOV treatment appeared to increase the colocalisation of FN and LRP1 in a dose dependent manner compared to untreated cells (Fig. 2). A diffuse staining pattern of Hsp90 was observed in all NOV treatments (Fig. 3) and there was colocalisation between Hsp90 and LRP1 in both untreated and NOV treated MEF-1 cells as observed by yellow pixels in merged images. Furthermore, we demonstrate that LRP1 is internalised in both Hs578T and MEF-1 cells (Fig. 4) by co-staining with the endocytic marker, LAMP-1. In addition, in response to NOV treatment we observed an

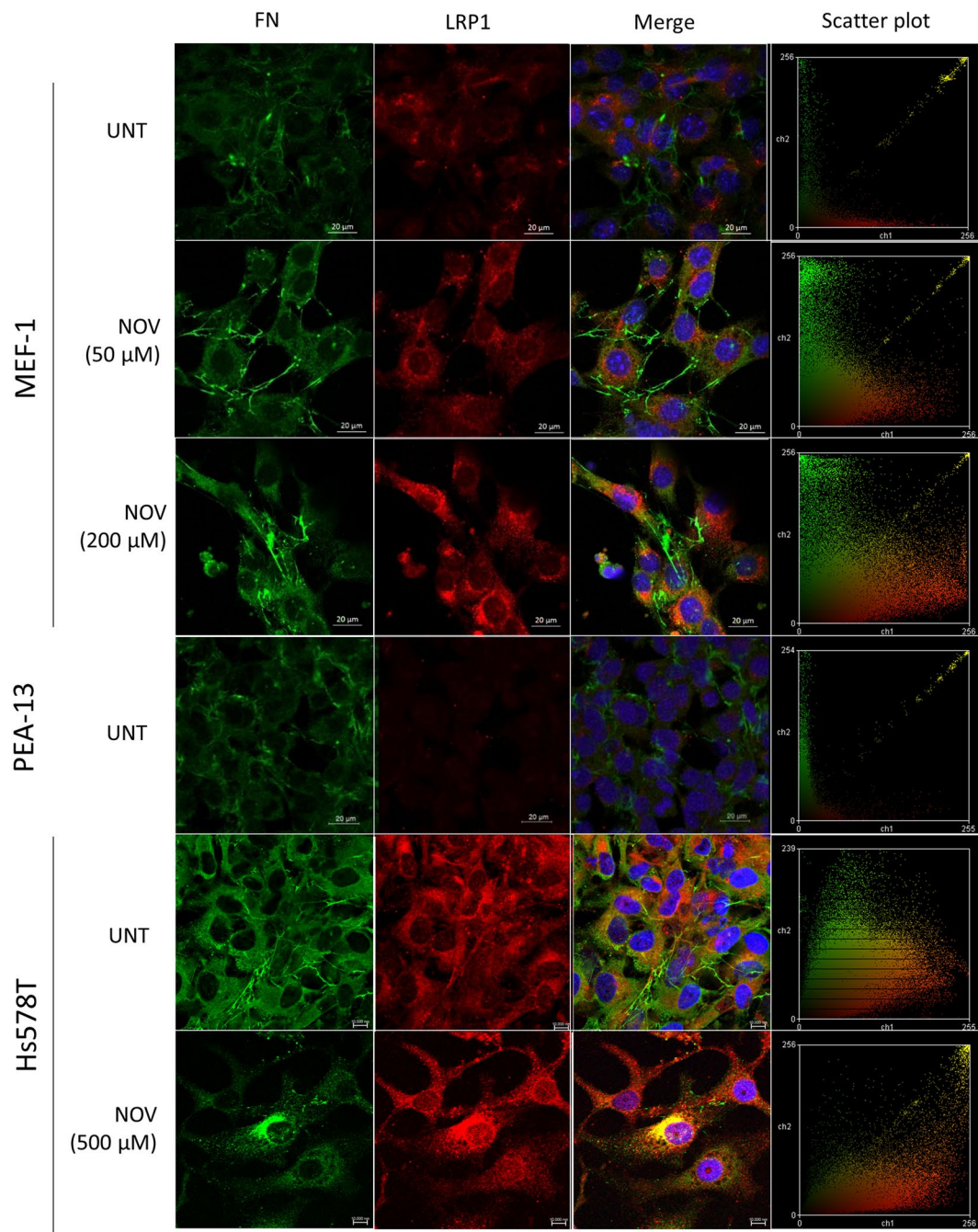


Figure 2. NOV treatment increased FN and LRP1 colocalisation in MEF-1 and Hs578T cells. Cells were treated with increasing concentrations of novobiocin (NOV) for 16 hours. Cells were fixed and incubated with mouse anti-FN (green) and rabbit anti-LRP1 (red) primary antibodies followed by donkey anti-mouse Alexa Fluor-488 and donkey anti-rabbit Alexa Fluor-546 respectively. Nuclei were stained with (1 µg/ml) Hoechst-33342 (blue). Images were captured using the 63x objective on the Zeiss LSM 780 Meta laser scanning confocal microscope and analyzed using Zen Blue software (Zeiss, Germany). Scatter plots were generated using Intensity Correlation Analysis plugin in ImageJ. Data are representative of images obtained from triplicate independent experiments with similar results. Scale bars represent 20 µm.

increase in the intensity of intracellular LRP1 staining and colocalisation with LAMP1 in both cell lines. Taken together, these data suggest that NOV treatment results in LRP1 endocytosis increasing colocalisation of LRP1 and FN and LRP1 and Hsp90 in lysosomes.

LRP1, Hsp90 and FN can be isolated in a common complex. LRP1 is known to bind Hsp90²⁵ and studies have demonstrated LRP1 to be a catabolic receptor for the uptake of FN²³. The association of Hsp90 with FN has previously been described by our group⁸. We therefore tested for a putative complex between Hsp90,

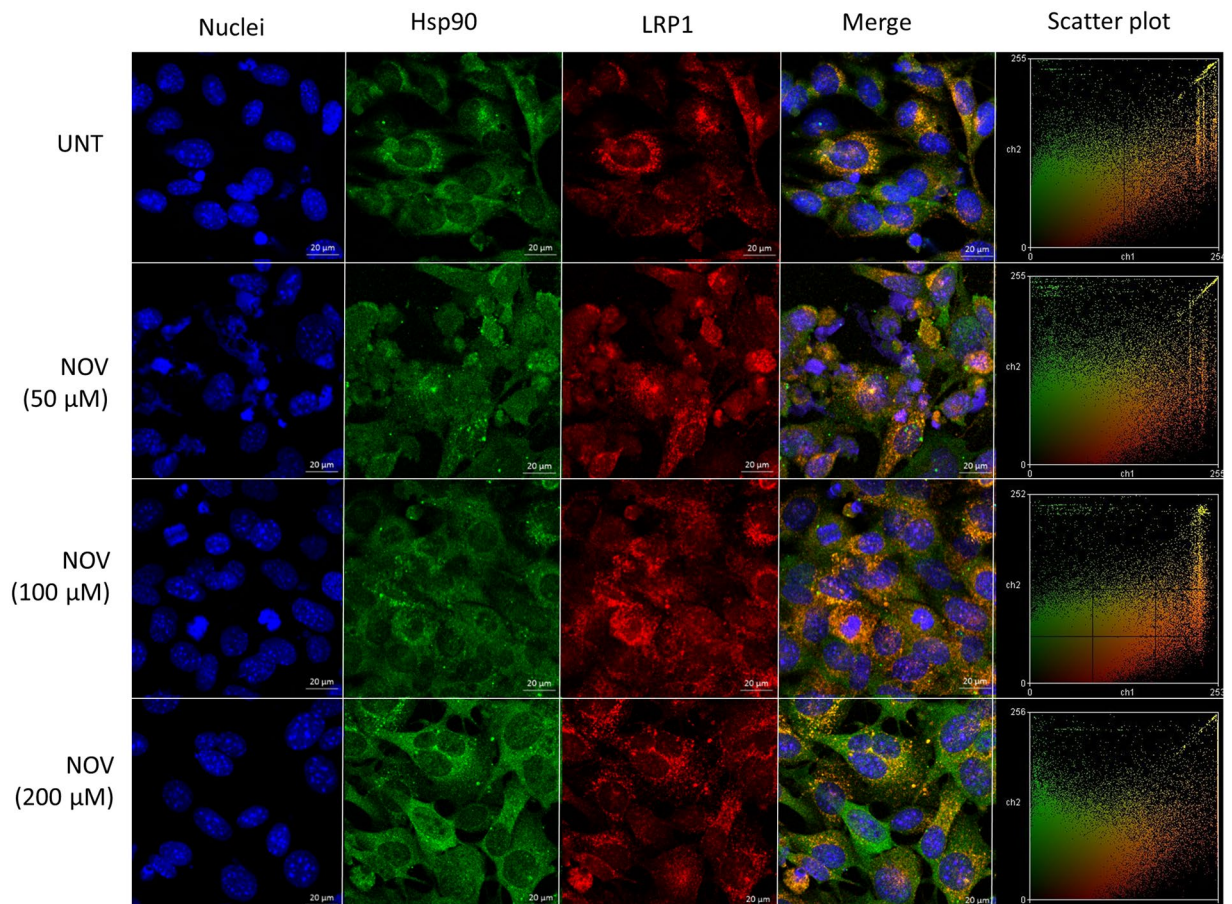


Figure 3. LRP1 and Hsp90 colocalise upon NOV treatment in MEF-1 cells. MEF-1 cells were treated with increasing concentrations of novobiocin (NOV) for 16 hours. Cells were fixed and incubated with goat anti-human Hsp90 α/β (green) and rabbit anti-human LRP1 (red) followed by donkey anti-goat Alexa Fluor-660 and donkey anti-rabbit Alexa Fluor-546. Nuclei were stained with (1 $\mu\text{g}/\text{ml}$) Hoechst-33342 (blue). Images were captured using the 63x objective on the Zeiss LSM 780 Meta laser scanning confocal microscope and analyzed using Zen Blue software (Zeiss, Germany). Scatter plots were generated using Intensity Correlation Analysis plugin in ImageJ. Data are representative of images obtained from triplicate independent experiments with similar results. Scale bars represent 20 μm .

LRP1 and FN (Fig. 5). We first showed that both MEF-1 and Hs578T cells express LRP1 and that levels of LRP1, unlike FN, are not affected by NOV treatment (Fig. 5A,B). NOV-treated and untreated MEF-1 and Hs578T cells were incubated with the cell-impermeable DTSSP crosslinker to covalently crosslink cell surface proteins and crosslinked LRP1 containing complexes isolated by immunoprecipitation (Fig. 5). LRP1 co-immunoprecipitation showed that Hsp90 and FN occur in a common complex with LRP1 on the surface of MEF-1 and Hs578T cells (Fig. 5C,D) in agreement with the colocalisation of FN, LRP1 and Hsp90 observed in the confocal analysis (Figs 2 and 3). In the immunoblot for FN in MEF-1 cells (Fig. 5C), immunoblotting for LRP1 showed similar levels of LRP1 (85 kDa) confirming that equal amounts of LRP1 were isolated in both fractions. The absence of proteins detected in the IgG IP elution fractions confirmed there were no non-specific binding of proteins. Upon overexposure, similar levels of Hsp90 were detected in both the NOV (N) and untreated (U) fractions as quantified in bar graphs below (Fig. 5C). The bands below Hsp90 represent non-specific binding. Treatment of Hs578T cells revealed similar results (Fig. 5D). Untreated and NOV treated lysates yielded similar levels of FN and Hsp90 immunoprecipitated with LRP1 (Fig. 5D). These data support the presence of a common complex containing Hsp90, LRP1 and FN in both Hs578T and MEF-1 cells that exists in both the absence and presence of NOV.

LRP1 blocking antibody recapitulated the effect of NOV on the FN matrix and was rescued by Hsp90 β .

Having shown that FN, LRP1 and Hsp90 can be isolated in a common complex, the effect of a commercial monoclonal LRP1 blocking antibody [8G1] on the FN matrix was compared to NOV treatment (Fig. 6). This antibody is reported to bind the 515 kDa alpha chain of LRP1 and prevent ligand binding^{20,37}. Treatment of Hs578T cells with the LRP1 blocking antibody (Fig. 6; mLRPab) showed a significant ($p < 0.001$) loss of extracellular FN in comparison to the untreated control (UNT) and was similar to NOV treatment (Fig. 6). The addition of exogenous Hsp90 β was able to significantly overcome the observed FN phenotype in mLRPab treated Hs578T cells ($p < 0.05$) and restored the extracellular FN matrix phenotype of mLRPab treated Hs578T cells similar to that of

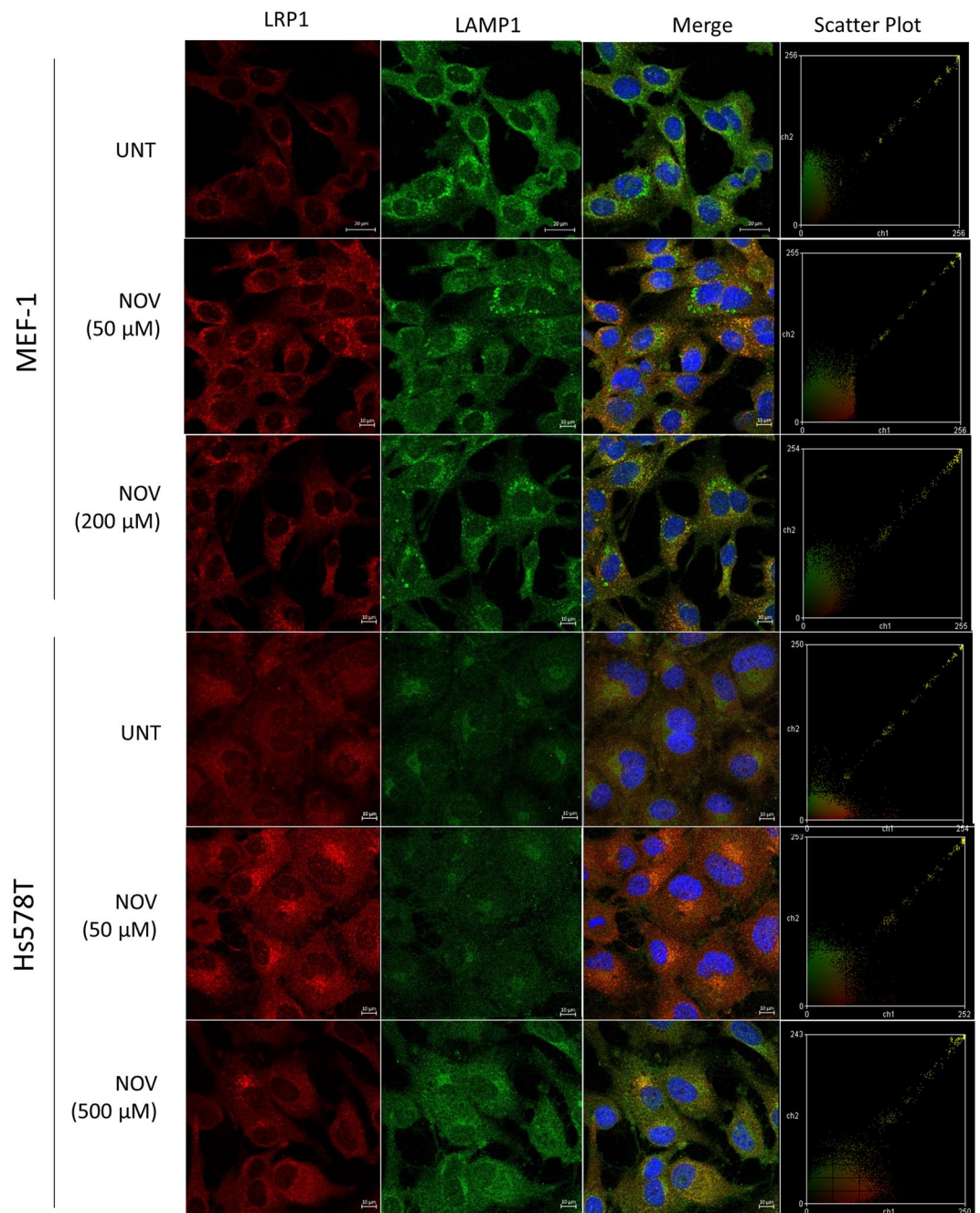


Figure 4. NOV treatment increased LRP1 and LAMP1 colocalisation in MEF-1 and Hs578T cells. Cells were treated with increasing concentrations of novobiocin (NOV) for 16 hours. Cells were fixed and incubated with rabbit anti-LRP1 (red) primary antibody followed by donkey anti-rabbit Alexa-fluor-488 and mouse anti-LAMP1 Alexa Fluor 630 (green). Nuclei were stained with (1 μ g/ml) Hoechst-33342 (blue). Images were captured using the 63x objective on the Zeiss LSM 780 Meta laser scanning confocal microscope and analyzed using Zen Blue software (Zeiss, Germany). Scatter plots were generated using Intensity Correlation Analysis plugin in ImageJ. Data are representative of images obtained from triplicate independent experiments with similar results. Scale bars represent 20 μ m.

the untreated control (Fig. 6, mLRPab + Hsp90). Treatment with a combination of NOV, mLRPab and exogenous Hsp90 β resulted in a loss of extracellular FN similar to that of NOV and mLRPab treated Hs578T cells, which support the fact that Hsp90 β was responsible for restoring the extracellular FN matrix phenotype due to the mLRPab (Fig. 6).

Loss of extracellular FN in response to NOV is dependent on the presence of LRP1. MEF-1 and PEA-13 cells were treated with increasing doses of NOV (0–1000 μ M) and samples were processed for western analysis (Fig. 7A). Immunoblotting for FN revealed that MEF-1 cells had significantly increased total FN

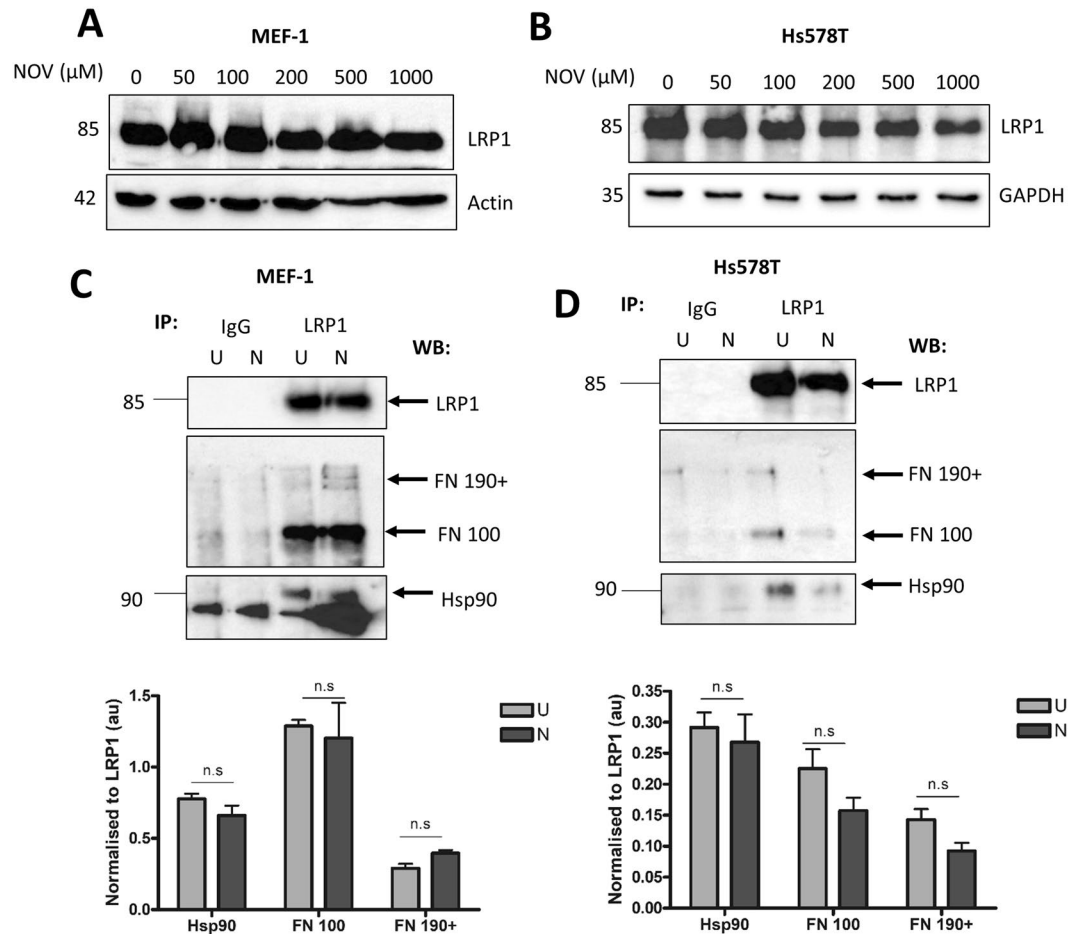


Figure 5. Hsp90, LRP1 and FN occur in a common complex in MEF-1 and Hs578T cells. (A) MEF-1 and (B) Hs578T lysates were treated with NOV and probed for LRP1 using rabbit anti-LRP1 antibodies. Actin or GAPDH were used as loading controls respectively. (C) MEF-1 and (D) Hs578T cells were left untreated (U) or treated with 50 μM NOV (N) for 16 hours. Extracellular proteins were crosslinked with the cell-impermeable crosslinker, DTSSP, and LRP1-containing complexes were isolated by immunoprecipitation (IP) with either LRP1 or isotype control IgG antibodies. Elution fractions were resolved on a 10% SDS gel and probed for FN, LRP1 and Hsp90 using rabbit anti-FN, rabbit anti-LRP1 and mouse anti-Hsp90 primary antibodies respectively. Densitometry of expression levels of FN and Hsp90 were determined relative to the amount of LRP1 in each immunoprecipitation and are presented as bar graphs. Statistical analyses was performed using a one-way ANOVA with Bonferroni post-test. Data shown are representative of duplicate experiments with similar results.

levels upon NOV treatment at 50 μM, followed by a dose-dependent loss of FN at higher NOV concentrations (Fig. 7A). Comparatively, LRP1-deficient PEA-13 cells showed no significant changes in total FN levels at equivalent concentrations. Interestingly, in MEF-1 cells, we also detected lower molecular weight FN bands (85 kDa) at low NOV concentrations (Fig. 7A). We suspect these may represent either proteolytic or assembly fragments of FN which importantly were not observed in the PEA-13 cells (Fig. 7A). These results suggest that there is a dose-dependent loss of FN in LRP1-expressing (i.e. MEF-1) cells, while in LRP1-deficient cells total FN levels do not change. We further show that this change in FN is specific to C-terminal inhibition of Hsp90 by demonstrating that Hsp90 inhibition by geldanamycin (GA), a known N-terminal inhibitor (Fig. 7B) does not produce the same response as NOV. Unlike NOV, GA is also known to bind Grp94, the ER Hsp90 paralogue, so these data also verify that the effects observed are not due to Grp94 inhibition. We also tested another C-terminal Hsp90 inhibitor, SM253 (kindly provided by Shelli McAlpine, UNSW, Australia), which blocks the Hsp90 C-terminus allosterically through interaction with the M domain of Hsp90³⁸. We demonstrate that SM253 produces a significant dose-dependent loss in FN, similar to that observed for NOV but only in MEF-1 cells and not in the PEA13 cell line (Fig. 7C). The changes in total FN observed in the MEF-1 cells (Fig. 7A) could be due to changes in rates of FN synthesis or degradation. To confirm if NOV resulted in FN degradation, we tested the effect of blocking of proteasomal and lysosomal degradation pathways on levels of FN in these cell lines. Cells were treated with the proteasomal inhibitor, MG132, in the presence and absence of NOV for 16 hours before being lysed and analysed by western analysis (Fig. 8A). In both MEF-1 and PEA-13 cells, addition of MG132 in the presence of NOV caused no significant accumulation of FN relative to NOV or MG132 treatments alone. On the other hand, treatment of MEF-1 cells with the lysosomal inhibitor, chloroquine (+CLQ) (Fig. 8B) significantly

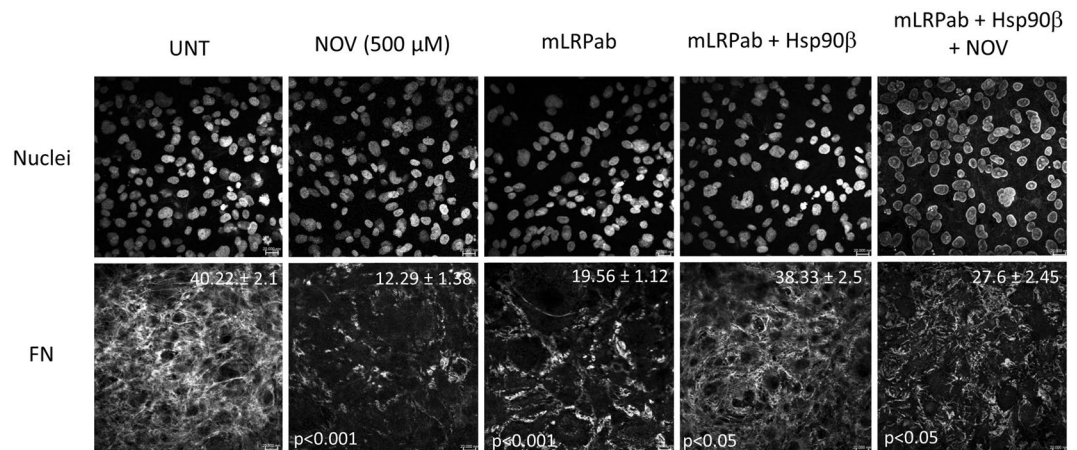


Figure 6. LRP1 blocking antibody induced loss of FN matrix which could be rescued by soluble Hsp90 β . Hs578T cells were treated with novobiocin (NOV; 500 μ M) for 1 hour at 37 $^{\circ}$ C followed by treatment with a blocking LRP1 antibody (mLRPab; 2 μ g/ml) for 10 minutes before addition of exogenous Hsp90 β (100 ng/ml) overnight. Fixed cells were stained using rabbit anti-human FN followed by donkey anti-rabbit DyLight[®] 488 fluorescent secondary antibodies. Nuclei were stained with Hoechst 33342 (1 μ g/ml). Images were captured using a Zeiss LSM 510 Meta laser scanning confocal microscope and analyzed using Zen software, blue edition (Zeiss, Germany). Scale bars are equivalent to 20 μ m. Values (in white) at the top of each frame represent the mean grey values per nuclei \pm SD (n = 3) for each treatment. Mean grey values were compared using a one-way ANOVA with a Tukey Post Test comparing all values. The mean grey value of NOV and LRP1 blocking antibody (mLRPab) treatments were compared to untreated cells. The mean grey value of LRP1 blocking antibody and exogenous Hsp90 β treated (mLRPab + Hsp90 β) cells were compared to the equivalent treatment without exogenous Hsp90 β (mLRPab). The mean grey value of a combination of all three treatments (NOV + mLRPab + Hsp90 β) was compared to untreated cells. Statistical p-values are shown in the bottom left of each frame. The data shown are representative of triplicate images collected from duplicate independent experiments.

increased levels of FN compared to control cells (–CLQ) in both untreated and NOV treated cells. There was no significant increase in FN levels in response to lysosomal inhibition in PEA13 cells. ECM proteins are known to be internalised by receptor mediated endocytosis and degraded in lysosomes³⁹. Evidence of FN turnover through its endocytosis and lysosomal degradation have been demonstrated²³, whilst protease inhibitors were shown to be unable to inhibit FN turnover⁴⁰. Supporting studies have also demonstrated the proteasomal inhibitor to be ineffective in preventing degradation of FN⁴¹. Given that the main proteolytic pathway for intracellular proteins is the proteasome, while extracellular proteins are predominantly processed by the lysosome⁴², taken together these data could suggest that the observed loss of FN in NOV treated MEF-1 cells (Fig. 7A) is due to internalization and degradation of extracellular FN in the lysosome. These data are consistent with the colocalisation of LRP1 and LAMP1 in NOV treated cells. In order to assess the effect of Hsp90 inhibition on FN protein stability, we performed a time course measurement of FN levels in MEF-1 cells when translation was blocked with cycloheximide (CHX)⁴³. MEF-1 cells were treated with CHX in the presence (+NOV) and absence (–NOV) of NOV for the indicated time periods (Fig. 8C). When translation of FN was blocked, a loss in total FN protein levels occurred earlier in NOV treated cells (+NOV) over 12 hours compared to the untreated control (–NOV). When compared with the control (–NOV) where FN levels appear stable with a noticeable loss observed only after 12 hours with CHX alone, levels of FN in NOV and CHX treated lysates were reduced after as little as 0.5 hrs and continued to reduce over the time course of the experiment (Fig. 8C). Additionally, mRNA levels of FN were not significantly altered during NOV treatments (data not shown). Taken together, these data suggest that the dose dependent decrease in total FN levels of MEF-1 cells above 50 μ M NOV (Fig. 8C) was most likely due to enhanced turnover of the protein.

NOV-induced loss of FN is largely extracellular FN matrix. In an attempt to identify whether the loss of total FN observed was due primarily to changes in the extracellular insoluble levels of FN, we employed two different assays to isolate this fraction of FN. First, a DOC assay was performed (Fig. 9A) in order to fractionate DOC-soluble (cell-associated) and DOC-insoluble (matrix-associated) FN pools⁴⁴. These fractions were probed for FN by western analysis and revealed increased levels of both insoluble and soluble FN in PEA-13 cells in comparison to MEF-1 cells (Fig. 9A). Upon NOV treatment, the insoluble FN in the LRP1-expressing MEF-1 and Hs578T cells increased at low NOV concentrations (i.e. 50 μ M) followed by a decrease to levels below that of the untreated control. The soluble levels of FN in this cell line also decreased in a dose dependent manner. There was no change in the insoluble FN levels of PEA-13 cells suggesting a resistance to extracellular FN loss in response to NOV treatment. Only at the highest concentration (2 000 μ M NOV) was the insoluble FN fraction lost. Soluble FN levels were stable up to 200 μ M, after which there was a dose dependent decrease (Fig. 9A). These data suggest

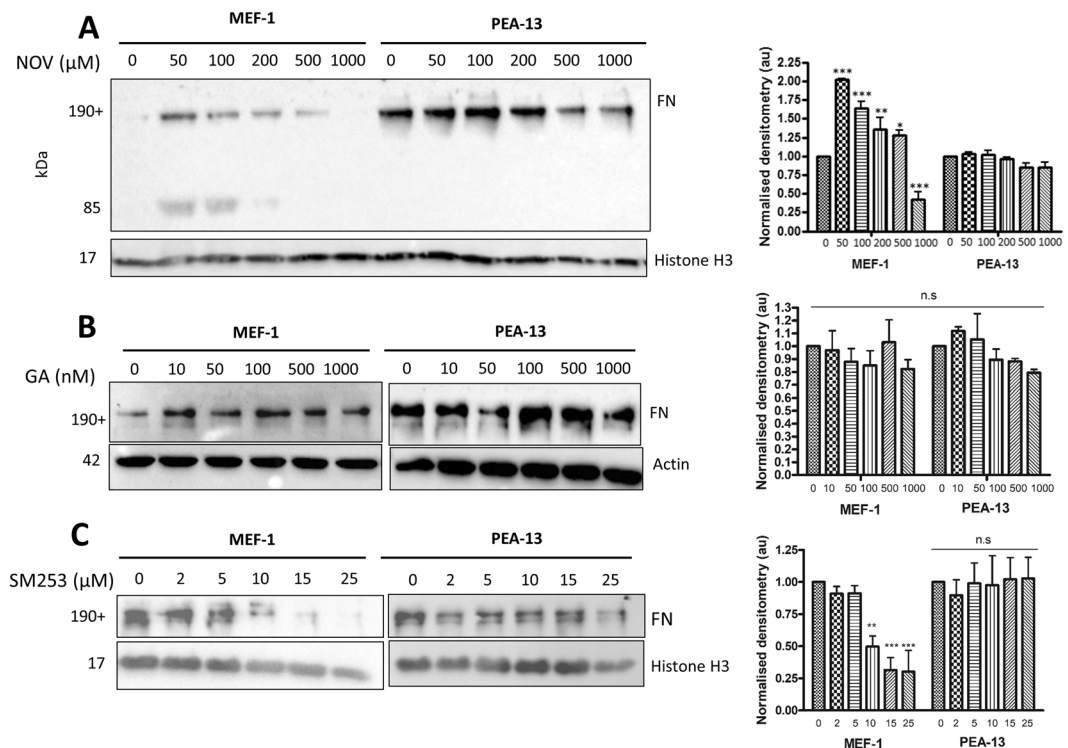


Figure 7. Loss of FN is specific to C-terminal Hsp90 inhibition in LRP1-expressing cells. **(A)** Adherent MEF-1 and PEA-13 were treated with increasing concentrations of novobiocin (NOV), **(B)** geldanamycin (GA) or **(C)** SM253 for 16 hours at 37 °C. Cells were lysed and equal amounts of total protein (50 μg) were probed for levels of FN using rabbit anti-FN primary antibodies. Histone H3 and actin were used as a loading controls. The densitometry represented alongside was determined using ImageJ. Statistical significance was determined using a two-way ANOVA in GraphPad Prism 4 (* $p < 0.05$, ** $p < 0.01$, *** $p < 0.001$). Error bars indicate \pm SD ($n = 3$).

that NOV treatment induces the loss of insoluble extracellular FN in LRP1-expressing MEF-1 and Hs578T cells, but not in LRP1-deficient PEA-13 cells.

In the second assay, we used a biotin-streptavidin purification to isolate extracellular surface proteins which had been biotinylated (Fig. 9B). MEF-1 and PEA-13 cells were treated with or without NOV (200 μM) before cell surface proteins were labelled by biotin tagging with the cell impermeable EZ-link NHS-biotin⁸. Figure 9B shows the western analysis of the affinity purified fractions with (+) and without (−) NOV and/or trypsin treatment (to demonstrate that extracellular fractions were isolated). The biotinylated MEF-1 fractions revealed reduced levels of FN in (+NOV) samples compared to (−NOV) samples. Equivalent control fractions which had been trypsin treated resulted in an almost complete loss of biotinylated FN. LRP1 levels were also reduced in response to trypsin treatment confirming that surface proteins were being isolated (Fig. 9B). Biotinylated PEA-13 fractions revealed increased surface FN in NOV-treated samples compared to (−NOV). Interestingly, affinity purified FN in PEA-13 cells appeared to be more resistant to trypsin treatment (+trypsin) in comparison to MEF-1 cells and in fact displayed higher levels of FN than the (−trypsin) fractions. The increased resistance of LRP1-deficient cells to trypsin detachment has been noted by others⁴⁵.

The loss of extracellular FN was confirmed by confocal microscopy. Untreated Hs578T (Fig. 10A), MEF-1 and PEA-13 (Fig. 10B) cell lines had a distinct FN fibrillar network in the extracellular space between neighbouring cells (indicated by white arrows). Low concentrations of NOV (i.e. 50 μM) appeared to maintain, and perhaps even enhance, the appearance of an extracellular FN matrix in LRP1 expressing Hs578T (Fig. 10A) and MEF-1 (Fig. 10B) cells. In Hs578T cells (Fig. 10A), upon higher NOV treatments (200 μM and 500 μM), the matrix was almost entirely lost appearing more intracellular (red arrows), with a concomitant appearance of vesicle-like structures within these cells as depicted in the magnified image (Fig. 10A). Treatment with NOV at higher concentrations in MEF-1 cells revealed a substantial loss of FN matrix (white arrows) with a concomitant increase in intracellular FN (red arrows) (Fig. 10B). PEA-13 cells did not lose their extracellular FN matrix as readily as the MEF-1 cells in response to NOV and some extracellular FN is seen to be retained even at the highest NOV concentration (Fig. 10B).

Collectively these data demonstrate that LRP1-deficient PEA-13 cells have high levels of extracellular FN matrix which is largely insoluble and does not readily decrease upon Hsp90 inhibition with NOV, whilst LRP1-expressing MEF-1 cells have comparatively less extracellular FN, which is more readily internalised upon Hsp90 inhibition.

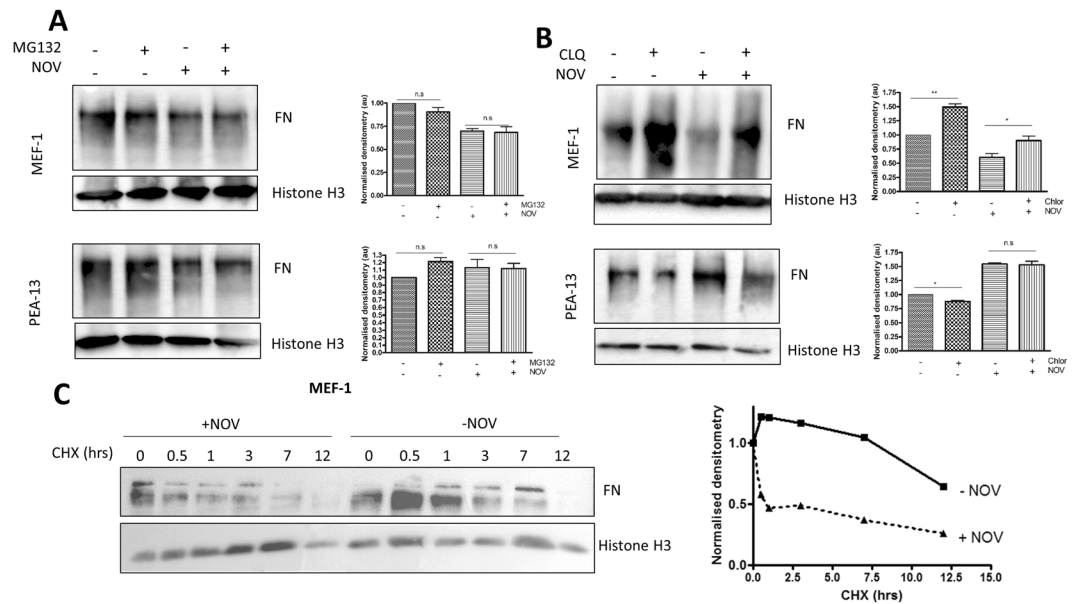


Figure 8. Effect of Hsp90 inhibition on the degradation of FN in MEF-1 and PEA-13 cells. MEF-1 and PEA-13 cells were treated (A) with (+) or without (–) MG132 (5 μ M) and (B) with (+) or (–) without chloroquine (CLQ) (100 μ M) in the presence or absence of 200 μ M NOV for 16 hours before lysing and probing for levels of FN. Statistical significance was determined by an unpaired two-tailed Student's t-test in GraphPad and is shown in bar graphs alongside. (C) MEF-1 cells were treated with 100 μ g/ml cycloheximide (CHX) in the presence or absence of novobiocin (NOV 200 μ M) and lysates prepared at the indicated time points. Equal amounts of total protein were probed for FN on a western blot with rabbit anti-FN antibody. Histone H3 was used as a loading control. The associated densitometry was determined using ImageJ software and is presented alongside. Data are representative of triplicate independent experiments.

Discussion

The ECM is highly dynamic and is constantly being remodelled to accommodate both physiological and pathological activities^{3,46}. Tissue homeostasis requires a balance between ECM synthesis and degradation. Any stimulus which perturbs homeostasis may result in progression of various disease states including fibrosis, cancer and other developmental abnormalities^{47,48}. We previously identified FN as a client of Hsp90 as it directly binds to Hsp90 and is dependent on Hsp90 for stability and conformational regulation⁸. In Hs578T cells, inhibition of Hsp90 with NOV led to a destabilisation of the FN matrix resulting in FN internalisation. The addition of exogenous Hsp90 β and/or endocytosis inhibitors was able to rescue the effect of NOV on FN (Fig. 1)⁸. We and other authors have previously reported that levels of extracellular Hsp90 in breast, colon and brain cancer cell lines range from approximately 5–20 ng/ml per 10^6 cells^{27,49}. Therefore, the concentrations used in our assays represent between 5–20 fold above the published endogenous levels. To better understand the mechanism of Hsp90-mediated FN internalisation, our current data extend this study and suggest that Hsp90 is involved in processes which maintain the stability of the extracellular FN matrix for which LRP1 mediates the clearance upon destabilisation or inhibition by NOV. To the best of our knowledge, this is the first report to investigate Hsp90 inhibition on FN turnover in MEFs and to link a dual role for Hsp90 and LRP1 in the turnover of FN. LRP1 exists in different pools in the cell, some will be intracellular (during synthesis or endocytosis) whilst the mature protein will be expressed on the cell surface. LRP1 has an extracellular region which comprises its ligand binding domains. LRP1 is known to endocytose and degrade a number of extracellular proteins including thrombospondins and plasminogen activators^{50,51} and functions as a receptor for extracellular Hsp90. Upon ectopic addition of Hsp90, it is able to bind the extracellular fragment of LRP1 and exert either cytokine like roles or chaperoning functions. Therefore, it is likely that Hsp90 (added ectopically) will interact with LRP1, as reported by others^{25,29,52}, followed by internalisation of this complex (with FN) during endocytosis which gives rise to the presence of LRP1 complexes intracellularly as observed in our study. It has also previously been reported that LRP1 is able to mediate FN internalisation and degradation²³. Here we show that LRP1 is required for the NOV-mediated turnover of extracellular FN.

The commercial monoclonal LRP1 blocking antibody used in our study binds the 515 kDa alpha chain of LRP1 and prevents binding of ligands³⁷. We anticipated that treatment with the blocking antibody would prevent FN endocytosis and result in an accumulation of extracellular FN matrix, however, this was not the case. Instead we found that the LRP1 blocking antibody caused a loss in FN matrix similar to that observed for NOV treatment, and which was rescued by exogenous Hsp90 β . FN matrix polymerization regulates the stability of FN matrix fibrils, and inhibitors of FN polymerization have been shown to diminish the amount of FN accumulating in the extracellular matrix⁵³. Our data might suggest a role for LRP1 in FN fibrillogenesis and/or stabilization of FN fibril assembly, in addition to the previously described role for LRP1 in FN catabolism²³. Irrespective of this, these data suggest that NOV treatment somehow leads to the inhibition of LRP1.

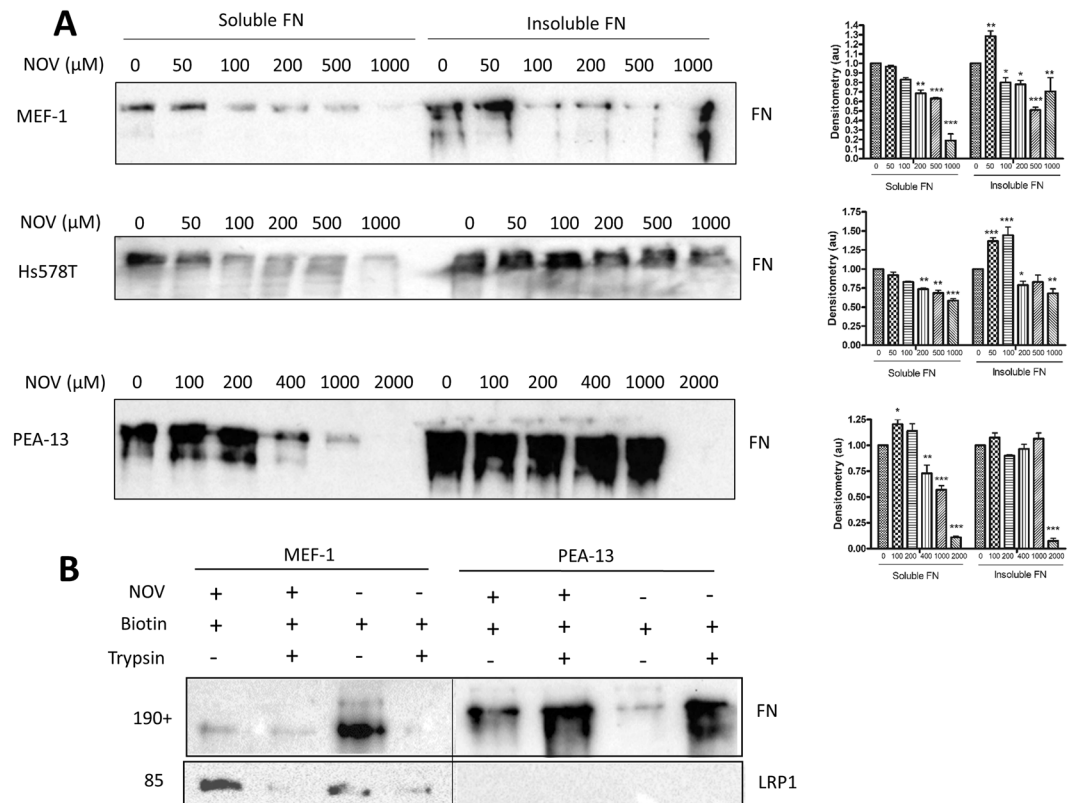


Figure 9. Loss of insoluble extracellular FN in response to NOV in MEF-1 not PEA-13 cells. **(A)** MEF-1, Hs578T and PEA-13 cells were treated with increasing doses of novobiocin (NOV) for 16 hours at 37 °C. Equal numbers of cells were harvested and the soluble and insoluble FN fractions separated using the DOC assay (Brenner *et al.*⁴⁴). FN levels were detected by immunoblotting with rabbit anti-human FN antibody. Densitometry values of the band intensities as determined in ImageJ are indicated in bar graphs representing duplicate experiments presented alongside. Statistical significance was determined compared to the untreated control by a two-way ANOVA with Bonferroni post-test in GraphPad Prism 4 (* $p < 0.05$, ** $p < 0.01$, *** $p < 0.001$). **(B)** MEF-1 and PEA-13 cells were treated for 16 hours with novobiocin (NOV 200 μ M) or left untreated. Surface biotinylated proteins were purified by streptavidin affinity chromatography and biotinylated fractions from equal numbers of cells and the resultant lysates probed for the presence of FN and LRP1 by western analysis. The data shown are representative of triplicate independent experiments.

The mechanism by which NOV inhibits LRP1 remains to be determined. We showed that Hsp90 forms a common complex with FN and LRP1 on the surface of MEF-1 and Hs578T cells, which surprisingly was not perturbed by NOV. This suggests that regulation of FN turnover by LRP1 is not due to changes in this complex. It is possible that the effect may be indirect and as a result of altered downstream signalling cascades in response to NOV. Roles for Hsp90-LRP1 cross-membrane signalling has previously been reported, whereby binding of extracellular Hsp90 to LRP1 induced the activation of downstream signalling pathways involving Akt and mTOR²⁶ and NF κ B²⁸. Activation of Akt and NF κ B have been reported to increase expression of FN^{32,33} and promote FN matrix assembly by activation of integrins⁵⁴. We might then expect a scenario where Hsp90 inhibition disrupts the Hsp90-LRP1 induced Akt or NF κ B signalling to reduce FN expression leading to loss of the FN ECM. However, this interpretation was not supported by the observations in our study as FN mRNA levels did not substantially change upon NOV treatment in MEFs (data not shown), and the levels of soluble FN were reduced by proteolysis in NOV-treated cells. In addition, it is not immediately clear how downstream signalling by Hsp90-LRP1 could be affected given that there was no change in the association of these proteins. Roles for Hsp90-LRP1 mediated activation of MMPs have also been demonstrated^{31,48,55,56}. MMPs are known to degrade the ECM (including FN) and activation of these enzymes has been linked to increased cell invasiveness^{57,58}. However, we did not see an increase in MMPs (data not shown) upon NOV treatments in either cell lines, which suggests that this is not the mechanism.

There is still debate around whether Hsp90 functions as a chaperone in the extracellular space or acts rather as a signalling molecule. We hypothesize that Hsp90 may have roles in both intracellular stabilization of soluble FN destined for export and extracellular stabilization of insoluble FN matrix and/or assisting in matrix assembly by regulating signalling pathways as a potential cytokine. These pathways still need to be identified and investigation into the precise mechanisms by which Hsp90 and LRP1 regulates NOV-induced FN turnover is continuing. The ECM is highly dynamic and is constantly being remodelled in both normal and diseased states. The functional relevance of the FN matrix and its turnover, in particular whether it serves to promote cell invasiveness by

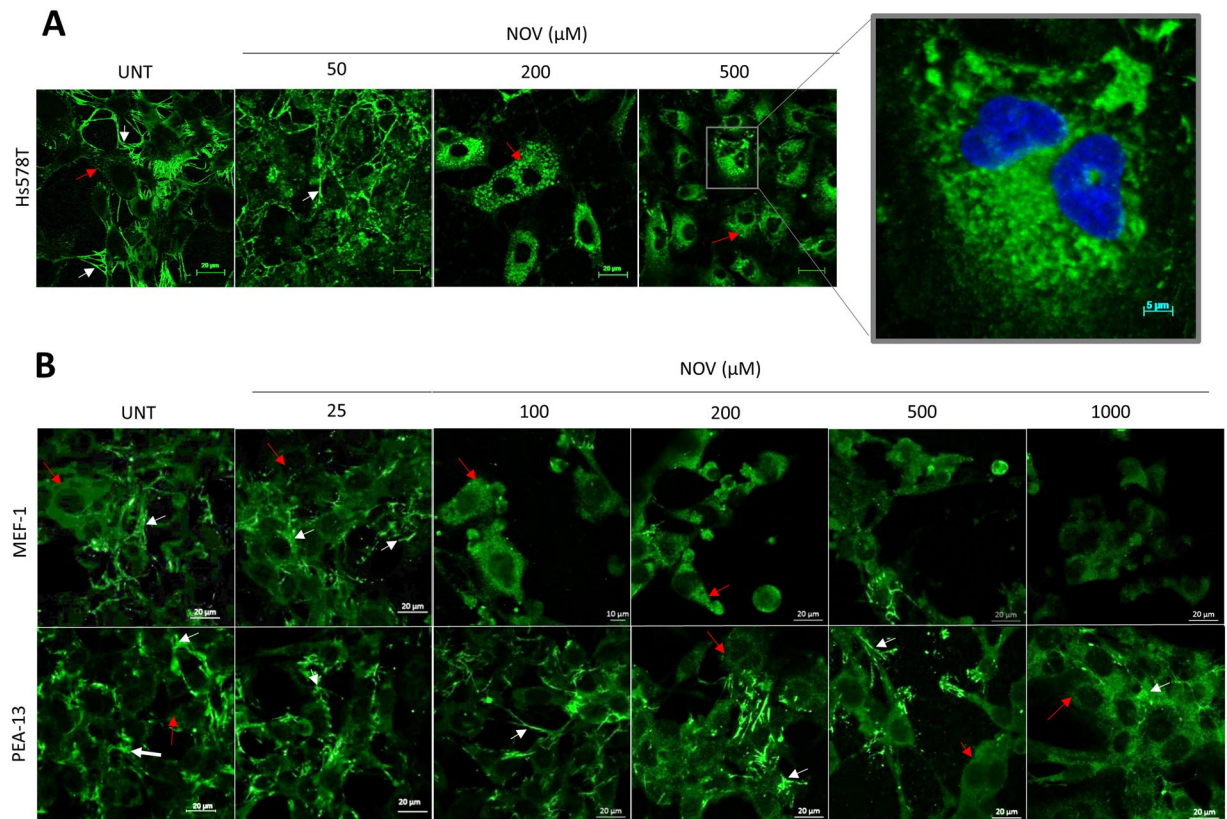


Figure 10. NOV induces internalisation of fibronectin matrix in LRP1-expressing Hs578T and MEF-1 cells but not LRP-deficient PEA13 cells. Cells were allowed to adhere overnight in a glass bottomed 15 well ibidi microdish and were treated with increasing concentrations of NOV in (A) Hs578T cells (0–500 μ M) and (B) MEF-1 and PEA-13 cells (0–1000 μ M) for 16 hours at 37 °C. Cells were fixed with ethanol and incubated with mouse primary antibody against FN (ab194395) followed by donkey anti-mouse Alexa Fluor-488. Images were captured using the Zeiss LSM 780 Meta laser scanning confocal microscope with the 63x oil objective and analysed using Zen Blue software. White arrows indicate extracellular FN matrix or FN fibrils and red arrows indicate intracellular FN. Scale bars represent 20 μ m. The data shown are representative of results obtained from triplicate experiments in all cases.

providing a scaffold on which to migrate, or acts as a barrier to migration, is an ongoing debate. However, it is clear that changes in the FN ECM are associated with pathology. The fact that certain Hsp90 inhibitors, which are intended for clinical use, cause deregulation of FN via a receptor that is ubiquitously expressed, means that these inhibitors may induce unintended ECM remodelling in a range of cell types which could ultimately culminate in disease. Further investigation is currently underway, but we have preliminary evidence which demonstrates an increased ability of LRP1-expressing cells to migrate at certain concentrations of NOV, suggesting putative physiological consequences associated with FN remodelling due to Hsp90 inhibition.

Methods

Antibodies. Mouse monoclonal anti-human Hsp90 α/β (cat no.: sc-13119) and goat polyclonal anti-human Hsp90 α/β (cat no.: sc-1055) primary antibodies were from Santa Cruz Biotechnology (USA). Mouse anti-human fibronectin (cat no.: F0916), rabbit anti-human fibronectin (cat no.: F3648), rabbit anti-human actin (cat no.: A2103) primary antibodies and goat anti-mouse IgG-HRP (cat no.: A2304) secondary antibody were from Sigma Aldrich (Germany). Rabbit monoclonal anti-human LRP1 (ab92544), mouse monoclonal [TV.1] anti-human fibronectin (ab194395), rabbit polyclonal anti-human histone H3 (ab1791) primary antibodies and donkey anti-rabbit IgG-HRP (ab16284) secondary antibody were from Abcam (UK). Donkey anti-mouse Dylight[®] 488 (ab96875), donkey anti-rabbit Dylight[®] 555 (ab96892) and donkey anti-goat Dylight[®] 650 (ab96934) secondary antibodies were also from Abcam (UK). Mouse monoclonal anti-human LRP1 blocking antibody (GTX79843) was from GeneTex (USA). Alexa Fluor-488 conjugated donkey anti-mouse IgG (cat no.: A21202), Alexa Fluor-546 conjugated donkey anti-rabbit IgG (cat no.: A10040), Alexa Fluor-660 conjugated donkey anti-goat IgG (cat no.: A21082) were from Invitrogen (UK).

Cell Culture. Hs578T (ATCC: HTB-126) breast cancer cell line and mouse embryonic fibroblasts (MEF) (i.e. LRP1 wild type MEF-1 [ATCC: CRL-2214] and LRP1 deficient PEA-13 [ATCC: CRL-2216]) were purchased from the American Type Culture Collection (ATCC). Hs578T breast cancer cells were maintained in Dulbecco's

Modified Eagle's Medium (DMEM) supplemented with 10% [v/v] FCS, 2 mM GlutaMAX™, 100 U/ml PSA and 2 mM insulin (Novorapid, Canada). Murine embryonic fibroblast lines (MEF) were maintained in DMEM supplemented with 10% [v/v] FCS, 2 mM GlutaMAX™ and 100 U/ml PSA. All cell lines were maintained at 37 °C in a humidified atmosphere with 9% CO₂.

SDS-PAGE and immunoblotting. Proteins were separated by discontinuous SDS-PAGE according to the modifications of the method described by Laemmli⁵⁹. Resolved proteins were transferred onto nitrocellulose membrane in western transfer buffer (25 mM Tris-Cl, 192 mM glycine, 20% [v/v] methanol) for 50 minutes at 0.4 A. Membranes were blocked for at least 1 hour at room temperature in 5% BLOTTO (5% [w/v] non-fat milk powder in Tris buffered saline [TBS: 50 mM Tris, 150 mM NaCl pH 7.5]). Membranes were incubated with primary antibody in 1% [w/v] BLOTTO at the recommended dilution overnight at 4 °C. Membranes were subsequently washed several times in TBST (TBS with 0.1% [v/v] Tween-20). Species matched secondary antibody conjugated to HRP was incubated with the membrane in fresh 1% [w/v] BLOTTO for 45 minutes at room temperature shaking after which the membranes were washed again in TBST at least four times. Proteins were detected using the ECL Advanced western blotting detection kit and visualised on the Chemidoc™ XRS system (BioRad). The full length Western blots for respective figures can be found in the Supplementary File.

Confocal Microscopy. Cells were seeded (3 × 10³ cells/well) into a 15-well ibidi plate and incubated overnight to allow cells to adhere. Cells were washed in phosphate buffered saline (PBS: pH 7.4; 137 mM NaCl, 27 mM KCl, 4.3 mM Na₂HPO₄, 4 mM KH₂PO₄), flash-treated with ice-cold ethanol and air dried. Cells were blocked with 1% [w/v] BSA/TBS and incubated with primary antibodies in 1% [w/v] BSA/TBS overnight at 4 °C. Cells were washed twice with 0.1% [w/v] BSA/TBS followed by 1 hour incubation with species specific fluorescently tagged secondary antibodies. Antibodies used are specified in figure legends. Nuclei were stained with Hoechst-33342 dye (Invitrogen) (1 µg/ml in distilled water). Images were captured using the Zeiss LSM780 Meta laser scanning confocal microscope and analyzed using Zen Blue Software.

Biochemical fractionation of insoluble and soluble fibronectin using a deoxycholate (DOC) assay. This assay was adapted from that published by Brenner and colleagues⁴⁴. MEF-1 and PEA-13 cells were seeded in a 6-well plate (6 × 10⁵ cells/well) and allowed to adhere overnight. Cells were treated with increasing concentrations of NOV for 16 hours and scraped into DOC buffer (2% [w/v] deoxycholate, 20 mM Tris-HCl, pH 8.8, 2 mM phenylmethanesulfonyl fluoride [PMSF], 2 mM EDTA and 0.05% [v/v] protease inhibitor cocktail). To separate soluble and insoluble fractions, the samples were vortexed for 2 minutes and centrifuged at 13000 rpm in a microfuge for 20 minutes at 4 °C. The supernatant containing soluble fibronectin was removed and the cell pellet containing insoluble fibronectin was resuspended in SDS sample buffer (1% [w/v] SDS, 25 mM Tris-HCl, pH 8.0, 2 mM PMSF, 2 mM EDTA and 0.05% [v/v] protease inhibitor cocktail).

Cell surface biotinylation and streptavidin affinity purification. Adherent MEF-1 and PEA-13 cells were treated for 16 hours with or without 200 µM NOV at 37 °C. Cell surface proteins were biotinylated by incubation with 1 mg/ml EZ-Link™ Sulfo-NHS-SS-Biotin in PBS (pH 8) for 1 hour at 4 °C and quenched in 1 M Tris-Cl (pH 7.5). Cells were washed twice in PBS to remove unbound NHS-biotin and lysed in radio-immunoprecipitation assay (RIPA) buffer (50 mM Tris-Cl, pH 7.4, 150 mM NaCl, 1 mM EDTA, 1 mM Na₃VO₄, 1% [v/v] Nonidet P-40 [NP40], 1 mM sodium deoxycholate, 1 mM PMSF, 0.05% [v/v] protease inhibitor cocktail) with gentle scraping. A second biotinylated flask (negative control) was lifted with trypsin/EDTA (to cleave surface protein interactions) followed by centrifugation at 2000 rpm for 2 minutes in a microfuge. Pelleted cells were resuspended in RIPA buffer. Biotinylated scraped or trypsinised cells were lysed for 30 minutes at 4 °C with gentle agitation. Lysates were cleared by centrifugation in a microfuge at 13000 rpm for 5 minutes at 4 °C and incubated with streptavidin conjugated agarose beads (Thermo Scientific, USA) for 1 hour at 4 °C. After centrifugation, the supernatant was discarded and purified proteins were released from the beads by boiling in 5x SDS sample buffer. Samples were resolved by SDS-PAGE and analysed by immunoblotting as described previously.

DTSSP cell surface crosslinking and immunoprecipitation of LRP1 containing complexes. Adherent cells were left untreated or treated with NOV as indicated in figure legends. Cells were washed twice in PBS and incubated with 3,3'-Dithiobis(sulfosuccinimidylpropionate) (DTSSP, 3 mg/ml) at 4 °C for 2 hours to allow for crosslinking of protein interactions followed by quenching with 1 M Tris-Cl (pH 7.5) at 4 °C for 15 minutes. Cells were lysed in ice cold non-denaturing buffer (20 mM Tris-Cl, pH 8, 137 mM NaCl, 1% [v/v] NP40, 2 mM EDTA, 0.05% [v/v] protease inhibitor cocktail) with gentle scraping. MagReSyn™ Protein A was bound to rabbit anti-human LRP1 primary antibody or an isotype control antibody according to manufacturer's instructions (ReSyn Biosciences, South Africa) and subsequently incubated with cleared lysates overnight at 4 °C. Beads in suspension were collected using a magnet and washed three times in wash buffer (50 mM Tris, pH 7, 150 mM NaCl, 1% [v/v] Tween 20) followed by a final wash in distilled water. LRP1 complexes were eluted from the beads by boiling in 5x SDS sample buffer containing β-mercaptoethanol to cleave DTSSP bound proteins from the LRP1 complex. Immunoprecipitated proteins were analysed by SDS-PAGE and immunoblotting as described.

Statistical analysis. Experiments were performed in triplicate unless otherwise stated and statistical analyses were conducted using either one-way or two-way ANOVA with Bonferroni post-test or unpaired two-tailed Students t-tests in GraphPad Prism Version 4 software.

Data availability. The datasets generated during and/or analysed during the current study are available from the corresponding author on reasonable request.

References

- Hynes, R. O. The extracellular matrix: not just pretty fibrils. *Science* (80-) **326**, 1216–1219 (2009).
- Cox, T. R. & Eler, J. T. Remodeling and homeostasis of the extracellular matrix: implications for fibrotic diseases and cancer. *Dis. Model. Mech.* **4**, 165–78 (2011).
- Bonnans, C., Chou, J. & Werb, Z. Remodelling the extracellular matrix in development and disease. *Nat. Rev. Mol. Cell Biol.* **15**, 786–801 (2014).
- Schwarzbauer, J. E. Fibronectin: from gene to protein. *Curr. Opin. Cell Biol.* **3**, 786–91 (1991).
- To, W. S. & Midwood, K. S. Plasma and cellular fibronectin: distinct and independent functions during tissue repair. *Fibrogenesis Tissue Repair* **4**, 21 (2011).
- Bridgewater, R. E., Norman, J. C. & Caswell, P. T. Integrin trafficking at a glance. *J. Cell Sci.* **125**, 3695–701 (2012).
- Singh, P., Carraher, C. & Schwarzbauer, J. E. Assembly of fibronectin extracellular matrix. *Annu. Rev. Cell Dev. Biol.* **26**, 397–419 (2010).
- Hunter, M. C. *et al.* Hsp90 Binds Directly to Fibronectin (FN) and Inhibition Reduces the Extracellular Fibronectin Matrix in Breast Cancer Cells. *Plos One* **9**, e86842 (2014).
- Taipale, M., Jarosz, D. F. & Lindquist, S. HSP90 at the hub of protein homeostasis: Emerging mechanistic insights. *Nat. Rev. Mol. Cell Biol.* **11**, 515–528 (2010).
- Taipale, M. *et al.* A quantitative chaperone architecture of Cellular Protein Homeostasis Pathways. *Cell* **158**, 434–448 (2014).
- Bagatell, R. & Whitesell, L. Altered Hsp90 function in cancer: A unique therapeutic opportunity. *Mol. Cancer Ther.* **3**, 1021–1030 (2004).
- Calderwood, S. K. Heat shock proteins and cancer: intracellular chaperones or extracellular signalling ligands? *Philosophical Transactions R. Soc. B* **373** (2017).
- Li, J., Soroka, J. & Buchner, J. The Hsp90 chaperone machinery: Conformational dynamics and regulation by co-chaperones. *Biochim. Biophys. Acta - Mol. Cell Res.* **1823**, 624–635 (2012).
- Zuehlke, A. D., Moses, M. A. & Neckers, L. Heat shock protein 90: its inhibition and function. *Philosophical Transactions R. Soc. B* **373** (2017).
- Sidera, K., Samiotaki, M., Yfanti, E., Panayotou, G. & Patsavoudi, E. Involvement of cell surface HSP90 in cell migration reveals a novel role in the developing nervous system. *J. Biol. Chem.* **279**, 45379–45388 (2004).
- McCready, J., Sims, J. D., Chan, D. & Jay, D. G. Secretion of extracellular hsp90 α via exosomes increases cancer cell motility: a role for plasminogen activation. *BMC Cancer* **10**, 1–10 (2010).
- Tsutsumi, S. *et al.* A small molecule cell-impermeant Hsp90 antagonist inhibits tumor cell motility and invasion. *Oncogene* **27**, 2478–2487 (2008).
- Li, W., Sahu, D. & Tsen, F. Secreted heat shock protein-90 (Hsp90) in wound healing and cancer. *Biochim. Biophys. Acta* **1823**, 730–41 (2011).
- Kounnas, M. Z. *et al.* LDL receptor-related protein, a multifunctional ApoE receptor, binds secreted beta-amyloid precursor protein and mediates its degradation. *Cell* **82**, 331–40 (1995).
- Strickland, D. K. *et al.* Sequence Identity between the α 2-Macroglobulin Receptor and Low Density Lipoprotein Receptor-related Protein Suggests That This Molecule Is a Multifunctional Receptor*. *J. Biol. Chem.* **265**, 17401–17405 (1990).
- Strickland, K. D., Kounnas, M. Z. & Argraves, S. LDL receptor-related for lipoprotein protein: a multiligand catabolism receptor and proteinase. *FASEB J.* **9**, 890–898 (1995).
- Rozañov, D. V., Hahn-Dantona, E., Strickland, D. K. & Strongin, A. Y. The Low Density Lipoprotein Receptor-related Protein LRP Is Regulated by Membrane Type-1 Matrix Metalloproteinase (MT1-MMP) Proteolysis in Malignant Cells. *J. Biol. Chem.* **279**, 4260–4268 (2004).
- Salicioni, A. M. *et al.* The Low Density Lipoprotein Receptor-related Protein Mediates Fibronectin Catabolism and Inhibits Fibronectin Accumulation on Cell Surfaces The Low Density Lipoprotein Receptor-related Protein Mediates Fibronectin. *J. Biol. Chem.* **277**, 16160–16166 (2002).
- Boucher, P. & Herz, J. Signaling through LRP1: Protection from atherosclerosis and beyond. *Biochem. Pharmacol.* **81**, 1–5 (2011).
- Basu, S., Binder, R. J., Ramalingam, T. & Srivastava, P. K. CD91 is a common receptor for heat shock proteins gp96, hsp90, hsp70, and calreticulin. *Immunity* **14**, 303–13 (2001).
- Tsen, F. *et al.* Extracellular heat shock protein 90 signals through subdomain II and the NPVY motif of LRP-1 receptor to Akt1 and Akt2: a circuit essential for promoting skin cell migration *in vitro* and wound healing *in vivo*. *Mol. Cell. Biol.* **33**, 4947–59 (2013).
- Gopal, U. *et al.* A Novel Extracellular Hsp90 Mediated Co-Receptor Function for LRP1 Regulates EphA2 Dependent Glioblastoma Cell Invasion. *Plos One* **6**, 1–14 (2011).
- Chen, J.-S. *et al.* Secreted heat shock protein 90 α induces colorectal cancer cell invasion through CD91/LRP-1 and NF-kappaB-mediated integrin α V expression. *J. Biol. Chem.* **285**, 25458–66 (2010).
- Cheng, C.-F. *et al.* Transforming growth factor α (TGF α)-stimulated secretion of HSP90 α : using the receptor LRP-1/CD91 to promote human skin cell migration against a TGF β -rich environment during wound healing. *Mol. Cell. Biol.* **28**, 3344–58 (2008).
- Hance, M. W., Nolan, K. D. & Isaacs, J. S. The Double-Edged Sword: Conserved Functions of Extracellular Hsp90 in Wound Healing and Cancer. *Cancers (Basel)*. **6**, 1065–1097 (2014).
- Song, H., Li, Y., Lee, J., Schwartz, A. L. & Bu, G. Low-Density Lipoprotein Receptor-Related Protein 1 Promotes Cancer Cell Migration and Invasion by Inducing the Expression of Matrix Metalloproteinases 2 and 9. *Cancer Res.* **69**, 879–887 (2009).
- Chen, W., Chen, C., Chen, L., Lee, C. & Huang, T. Secreted Heat Shock Protein 90 α (HSP90 α) Induces Nuclear Factor-kB-mediated TCF12 Protein Expression to Down-regulate E-cadherin and to Enhance Colorectal Cancer Cell Migration and Invasion*. *J. Biol. Chem.* **288**, 9001–9010 (2013).
- Qin, D., Zhang, G.-M., Xu, X. & Wang, L.-Y. The PI3K/Akt signaling pathway mediates the high glucose-induced expression of extracellular matrix molecules in human retinal pigment epithelial cells. *J. Diabetes Res.* **2015**, 1–11 (2015).
- Dong, H. *et al.* Breast Cancer MDA-MB-231 Cells Use Secreted Heat Shock Protein-90 α (Hsp90 α) to Survive a Hostile Hypoxic Environment. *Sci. Rep.* **6**, 20605 (2016).
- Willnow, T. E. & Herz, J. Genetic deficiency in low density lipoprotein receptor-related protein confers cellular resistance to Pseudomonas exotoxin A. Evidence that this protein is required for uptake and degradation of multiple ligands. *J. Cell Sci.* **107**, 719–726 (1994).
- Weaver, A. M., Hussaini, I. M., Mazar, A., Henkin, J. & Gonias, S. L. Embryonic Fibroblasts That Are Genetically Deficient in Low Density Lipoprotein Receptor-related Protein Demonstrate Increased Activity of the Urokinase Receptor System and Accelerated Migration on Vitronectin. *J. Biol. Chem.* **272**, 14372–14379 (1997).
- Scilabra, S. D. *et al.* Differential regulation of extracellular tissue inhibitor of metalloproteinases-3 levels by cell membrane-bound and shed low density lipoprotein receptor-related protein 1. *J. Biol. Chem.* **288**, 332–342 (2013).
- Koay, Y. C. *et al.* Chemically accessible hsp90 inhibitor that does not induce a heat shock response. *ACS Med. Chem. Lett.* **5**, 771–776 (2014).
- McKeown-Longo, P. J. & Mosher, D. F. Interaction of the 70,000-mol-wt amino-terminal fragment of fibronectin with the matrix-assembly receptor of fibroblasts. *J. Cell Biol.* **100**, 364–74 (1985).

40. Sottile, J. & Hocking, D. C. Fibronectin Polymerization Regulates the Composition and Stability of Extracellular Matrix Fibrils and Cell-Matrix Adhesions. *Mol. Biol. Cell* **13**, 3546–3559 (2002).
41. Ray, D., Osmundson, E. C. & Kiyokawa, H. Constitutive and UV-induced fibronectin degradation is a ubiquitination-dependent process controlled by β -TrCP. *J. Biol. Chem.* **281**, 23060–23065 (2006).
42. Ciechanover, A. Intracellular protein degradation: from a vague idea thru the lysosome and the ubiquitin – proteasome system and onto human diseases and drug targeting*. *Cell Death Differ.* **12**, 1178–1190 (2005).
43. Zhang, F., Snead, C. M. & Catravas, J. D. Hsp90 regulates O-linked beta-N-acetylglucosamine transferase: a novel mechanism of modulation of protein O-linked beta-N-acetylglucosamine modification in endothelial cells. *Am. J. Physiol. Cell Physiol.* **302**, 1786–1796 (2012).
44. Brenner, K. A., Corbett, S. A. & Schwarzbauer, J. E. Regulation of fibronectin matrix assembly by activated Ras in transformed cells. *Oncogene* **19**, 3156–3163 (2000).
45. Dedieu, S. *et al.* LRP-1 Silencing Prevents Malignant Cell Invasion despite Increased Pericellular Proteolytic Activities. *Mol. Cell. Biol.* **28**, 2980–2995 (2008).
46. Daley, W. P., Peters, S. B. & Larsen, M. Extracellular matrix dynamics in development and regenerative medicine. *J. Cell Sci.* **121**, 255–264 (2008).
47. Frantz, C., Stewart, K. M. & Weaver, V. M. The extracellular matrix at a glance The Extracellular Matrix at a Glance. *J. Cell Sci.* **2010**, 4195–4200 (2010).
48. Lu, P., Takai, K., Weaver, V. M. & Werb, Z. Extracellular matrix degradation and remodeling in development and disease. *Cold Spring Harb Perspect Biol* **3** (2011).
49. de la Mare, J.-A., Jurgens, T. & Edkins, A. L. Extracellular Hsp90 and TGF β regulate adhesion, migration and anchorage independent growth in a paired colon cancer cell line model. *BMC Cancer* **17**, 202 (2017).
50. Godyna, S. *et al.* Identification of the Low Density Lipoprotein Receptor-related Protein (LRP) as an Endocytic Receptor for Thrombospondin-1 Solid-phase Binding Assays. *J. Cell Biol.* **129**, 1403–1410 (1995).
51. Herz, J. & Strickland, D. K. Multiligand receptors LRP: a multifunctional scavenger and signaling receptor. *J. Clin. Invest* **108**, 779–784 (2001).
52. Woodley, D. T. *et al.* Participation of the lipoprotein receptor LRP1 in hypoxia-HSP90 α autocrine signaling to promote keratinocyte migration. *J. Cell Sci.* **122**, 1495–8 (2009).
53. Altmock, E. *et al.* Inhibition of fibronectin deposition improves experimental liver fibrosis. *J. Hepatol.* **62**, 625–633 (2014).
54. Somanath, P. R., Kandel, E. S., Hay, N. & Byzova, T. V. Akt1 Signaling Regulates Integrin Activation, Matrix Recognition, and Fibronectin Assembly. *J. Biol. Chem.* **282**, 22964–22976 (2007).
55. Hance, M. W. *et al.* Secreted Hsp90 Is a Novel Regulator of the Epithelial to Mesenchymal Transition (EMT) in Prostate Cancer. *J. Biol. Chem.* **287**, 37732–37744 (2012).
56. Sims, J. D., McCreedy, J. & Jay, D. G. Extracellular heat shock protein (Hsp)70 and Hsp90 α assist in matrix metalloproteinase-2 activation and breast cancer cell migration and invasion. *Plos One* **6**, e18848 (2011).
57. Stellas, D., El Hamidieh, A. & Patsavoudi, E. Monoclonal antibody 4C5 prevents activation of MMP2 and MMP9 by disrupting their interaction with extracellular HSP90 and inhibits formation of metastatic breast cancer cell deposits. *BMC Cell Biol.* **11**, 51 (2010).
58. Zhang, X., Chen, C. T., Bhargava, M. & Torzilli, P. A. A Comparative Study of Fibronectin Cleavage by MMP-1, -3, -13, and -14. *Cartilage* **3**, 267–277 (2013).
59. Laemmli, U. K. Cleavage of structural proteins during the assembly of the head of bacteriophage T4. *Nature* **227**, 680–685 (1970).

Acknowledgements

This research was supported by funding from the South African Research Chairs Initiative of the Department of Science and Technology (DST) and National Research Foundation of South Africa (NRF) (Grant No 98566), National Research Foundation CPRR (Grant No 105829), and Rhodes University. N.M.E.B. and M.C.H. were supported by postgraduate bursaries from the NRF and NRF/DAAD, respectively. The views expressed are those of the authors and should not be attributed to the DST, NRF, DAAD or Rhodes University.

Author Contributions

A.L.E. conceived of the study, A.L.E., N.M.E.B. and M.C.H. designed experiments; N.M.E.B. and M.C.H. conducted experiments; A.L.E. and N.M.E.B. analysed data and wrote the manuscript. All authors read and approved the final manuscript.

Additional Information

Supplementary information accompanies this paper at <https://doi.org/10.1038/s41598-018-29531-2>.

Competing Interests: The authors declare no competing interests.

Publisher's note: Springer Nature remains neutral with regard to jurisdictional claims in published maps and institutional affiliations.



Open Access This article is licensed under a Creative Commons Attribution 4.0 International License, which permits use, sharing, adaptation, distribution and reproduction in any medium or format, as long as you give appropriate credit to the original author(s) and the source, provide a link to the Creative Commons license, and indicate if changes were made. The images or other third party material in this article are included in the article's Creative Commons license, unless indicated otherwise in a credit line to the material. If material is not included in the article's Creative Commons license and your intended use is not permitted by statutory regulation or exceeds the permitted use, you will need to obtain permission directly from the copyright holder. To view a copy of this license, visit <http://creativecommons.org/licenses/by/4.0/>.

© The Author(s) 2018